Progress In Electromagnetics Research C, Vol. 87, 135–146, 2018

Partially Dielectric-Filled Empty Substrate Integrated Waveguide Design for Millimeter-Wave Applications

Karrar A. Khanjar* **and Tarek Djerafi**

Abstract—Partially dielectric-filled empty substrate integrated waveguide (PFESIW) is introduced for millimeter-wave application alongside partially dielectric-filled ESIW filter by using inverter and resonators technique. The new design presents good transition implementation in order to introduce a waveguide compatible with planar integrated circuits. The main goal of introducing the new transmission line PFESIW is to control characteristic impedance without changing the cutoff frequency. The presented transmission line is analyzed by calculating attenuation constant α, phase constant β and characteristic impedance Z. The PFESIW is used to build a resonator with high-quality factor. The filter based on the combination of of ESIW and PFESIW is proposed. Furthermore, the designed filter showed very good performance in terms of bandwidth and cost. Transmission line and filter prototypes are manufactured using standard printed circuit board fabrication. Partially dielectric-filled ESIW measurement displays very good results in terms of phase constant β, attenuation constant α, return loss (S_{11}) and insertion loss (S_{21}). Measured return loss (S_{11}) and insertion loss (S_{21}) for waveguide and filter agree very well with simulation.

1. INTRODUCTION

During the past decade, a lot of attention and effort have been devoted to improving an integrated circuit structure that can be integrated with the planar circuit. The invention of the substrate integrated waveguide (SIW) was a favourable start to realize the integration of the rectangular waveguide with RF circuits, which have caught considerable attention over the last decade [1]. This structure (SIW) offers a good performance in resonators and thus lower losses while maintaining low cost, small size, and easy manufacture. The drawback for SIW is a low-quality factor in comparison to traditional waveguide due to the propagation of the waves through a lossy dielectric material.

For the above-mentioned reasons, empty substrate integrated waveguide (ESIW) has been introduced to reduce the loss and get closer to the traditional waveguide in terms of quality factor's value. A proper transition between ESIW and microstrip was proposed in order to connect all parts of integrated circuits [2, 3]. Therefore, the quality factor is definitely higher. The drawback for ESIW is the large size of its structure which is close to the standard metrical waveguide. Furthermore, one of the major challenges for ESIW as well for the SIW is not only the large size but also controlling the impedance for a waveguide without modifying the cutoff frequency. In order to reduce the ESIW size and control the impedance, partially dielectric-filled ESIW is introduced.

The filter is one of the most important components of microwave systems since the massive majority of the microwave systems require filters to reject unwanted signals or to eliminate carried power in some frequency bands. Recently, bandpass filter by using ESIW structure was first introduced in [2]. The filter is meant to work at the centre frequency of 19.5 GHz and with 500-MHz bandwidth. Later on, many researchers have followed up the same trend to design filters via ESIW in [4–6]. On the other

Received 11 June 2018, Accepted 7 September 2018, Scheduled 30 September 2018
* Corresponding author: Karrar Al Khanjar (karrar.al.khanjar@emt.inrs.ca).
The authors are with the EMT Lab, Institut National De La Recherche Scientifique (INRS), Canada.

hand, dielectric loaded filter waveguide is a very good example of a filter waveguide with an acceptable quality factor. The first E-plane loaded dielectric filter is introduced by [7] which has a bandwidth from 9.5 to 10 GHz for a 5 poles bandpass filter with 0.1 dB ripples. Later on, biaxial discontinuities filter studied by [8] and discontinuity bandpass filter are designed at evanescent mode. The method of designing the filter is done by inserting E-plane dielectric loaded to the rectangular waveguide in order to make the waveguide working under cutoff frequency.

The method of dielectric loaded waveguide is adopted in [9] where analysis of inhomogeneously dielectric filled cavities coupled to dielectric-loaded waveguides is presented. In addition, analysis of loaded-waveguide of dielectric type is studied in [10]. In the literature, other attempts to design a waveguide by ESIW technology are experimented, such as E-plane technology used with ESIW in [11], multilayer ESIW with a versatile transition in [12], multilevel transition in ESIW [13], ESIW for power-handling [14], and ESIW for passive component circuit [15].

In order to further explore the advantages of empty substrate transmission lines, partially dielectric-filled ESIW waveguide and ESIW bandpass filter are presented. By utilizing empty substrate integrated waveguide (ESIW) structure and dielectric loaded filter technology, the possibility of controlling the impedance of waveguide without the need to modify the cutoff frequency is increased dramatically beside potential to reduce the size of ESIW. The designed filter and dielectric-filled ESIW are aimed to work at millimetres applications band. Bandpass filter ESIW model is studied by characterizing its parameters. The transmission line is modeled, which includes β and attenuation α calculations and measurements. This filter is designed and measured carefully to ensure the coupling between dielectric planes to create resonators suitable for millimetre applications where good transition technique is utilized to connect ESIW filter to microstrip for the planar substrate.

2. CHARACTERISTIC PARAMETERS OF TRANSMISSION LINE

Dielectric-filled waveguide considered here is limited to the case of one E-plane slabs placed symmetrically inside the waveguide. The considered geometry is a loaded rectangular waveguide with a dielectric slab placed across the center of the waveguide in the E plane. The normal mode in dielectric-loaded guides is TE_{10} mode of components normal to the dielectric interface. This corresponds to assuming the transverse direction to the interface normal vector to be the direction of propagation. In order to assign dielectric-filled technology inside ESIW, transmission line is adopted with a transition to fit ESIW technology. A 3D layout of transmission line structure and all dimensions is shown in Fig. 1. Discussion in this paper is based on ESIW and transmission line theory. The Rogers 6002 with

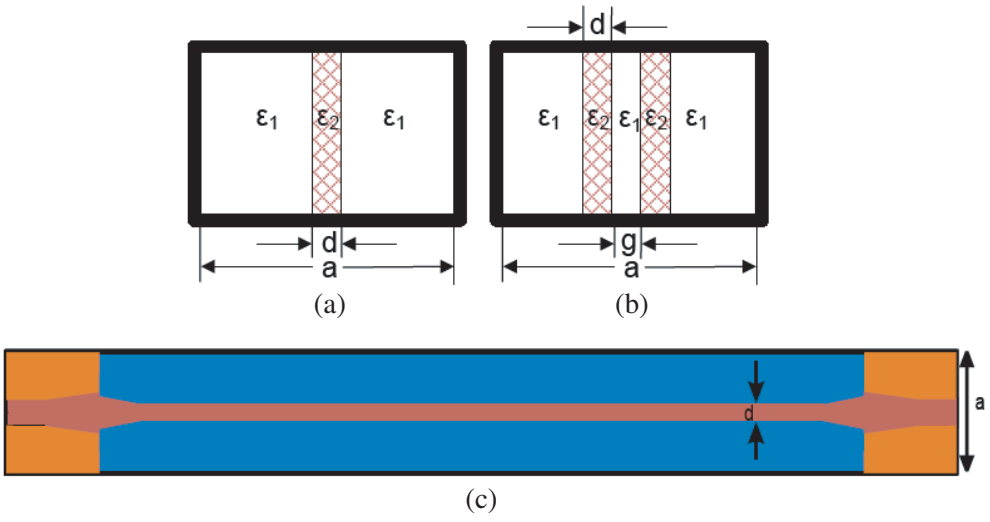

Figure 1. Partially dielectric-filled waveguide cross sectional view, (a) one dielectric slab, (b) two dielectric slab, (c) partially dielectric-filled ESIW with transition and microstrip transmission line, $d = 1.15$ mm, $a = 8$ mm.

permittivity of 2.94, thickness of 0.762 mm, loss tangent $\delta = 0.002$ and copper thickness of 17 µm is considered.

The analysis of characteristic parameters of this TL will be based on three important parameters β, α and Z.

2.1. Phase Constant

The phase constant β of transmission line waveguide is extracted from HFSS at a range frequency of 10–30 GHz. The waveguide width is chosen to be 8 mm, and d ranges from 0 to 8 mm where $d = 0$ mm is equivalent to the ESIW, and $d = 8$ mm is equivalent to standard SIW. Phase constant of this dielectric-filled ESIW waveguide changes proportionally to the dimension of the dielectric width d as demonstrated in Fig. 2. The shift in cutoff frequency happens due to an increase in dielectric width and accordingly will affect the phase constant. From Fig. 2, it can be noticed very clearly that changing the dimension of d actually varies the waveguide from ESIW to SIW based on the variation of d and thus β. The variation of λ_c is found when the width of d is changed as shown in Fig. 3. The variation is more important in the range above 4 mm equivalent to $a/2$.

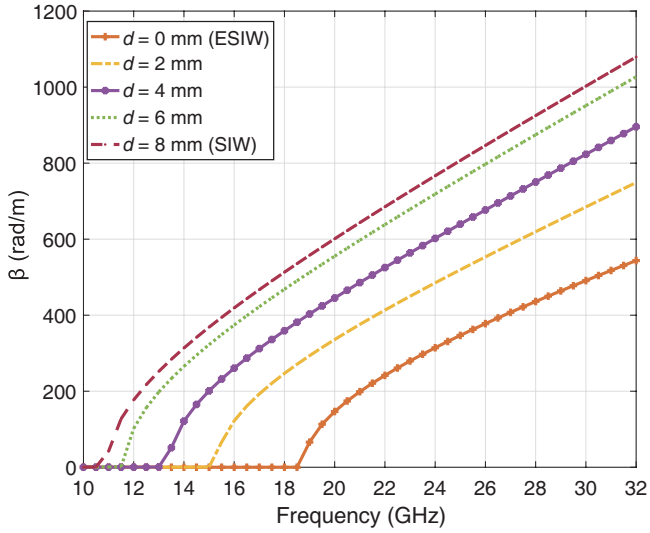

Figure 2. Phase constants of partially dielectric-filled ESIW solved by HFSS.

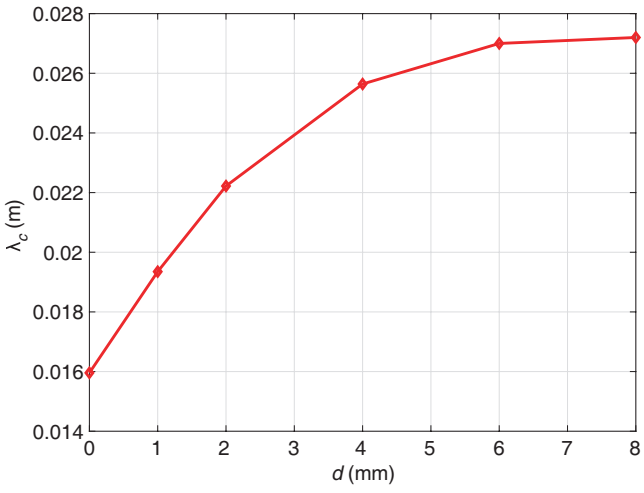

Figure 3. Wavelength for cut-off frequency with different value of (d) mm.

2.2. Attenuation Constant

The attenuation constant α of transmission line waveguide is calculated and extracted from HFSS at a range frequency of (10–30 GHz). The attenuation constant in the waveguide is a function of height h, the width of dielectric d (mm) and the width of the rectangular waveguide a [16]. Since the substrate has a fixed height, h for waveguide is fixed. In the case of ESIW, conductor loss is the main source for losses. In addition, small loss happens from dielectric as the transition is added. Therefore, the proper design concerning the ratio (a) is needed to reduce the loss to the minimum. As shown in Fig. 4, we analyze the attenuation constant of the waveguide when d is adjusted and a is fixed. The width of the waveguide is chosen to be 8 mm, and the dielectric width d ranges 1–8 mm.

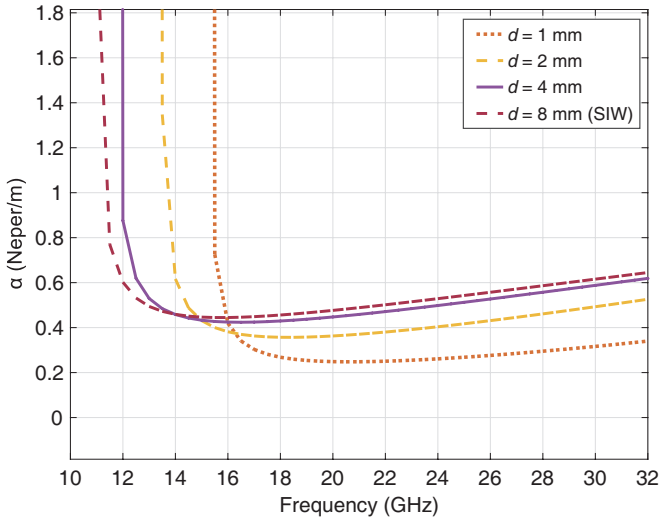

Figure 4. Attenuation variation with (d) for partially dielectric-filled ESIW extracted from HFSS.

As can be shown in Fig. 4, the wider d is, the smaller the attenuation constant is which is similar results to that found in [17]. It can be seen that by changing d size, the attenuation constant is varied from ESIW to SIW. The loss is almost the same as the SIW when $d = 4$ mm ($a/2$), and we observe the reduction of 30% when $d = 2$ mm ($a/4$).

2.3. Impedance

The characteristic impedance of a waveguide can be found from HFSS at a range frequency of (10–32 GHz). The waveguide width is chosen to be 8 mm, and d is ranges from 0 to 8 mm. Characteristic impedance is dropping down by increasing the width of dielectric T.L (d) which can be noticed at single-mode as illustrated in Fig. 5. These results show clearly that it is possible to control characteristic impedance by adjusting only the width of filled dielectric T.L (d) without the need to modify the waveguide parameters that control the cutoff frequency (width and height).

3. CIRCUIT TRANSITION

The transition from microstrip to ESIW is used to propagate the wave from the microstrip to empty waveguide. Some designs introduce sma connector to ESIW transition in [18]. The proposed transition is adopted from [2] and optimized to work with 50 Ω input of designed PFESIW. Transition is modified to fit dielectric-filled load in the middle of ESIW. Therefore, it has been connected directly to dielectric load in order to keep the propagating waves in the same dielectric material rather than transmitting the wave from the transition to ESIW and then to dielectric-filled load in centre of the waveguide. It is worth to mention that transition is optimized separately and attached to loaded filter in Section 5. Fig. 6

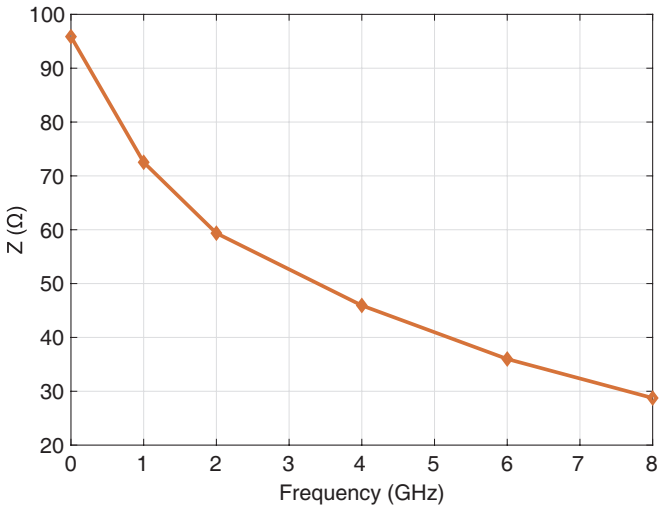

Figure 5. Characteristic impedance of a partially dielectric-filled ESIW extracted from HFSS with different value of dielectric-filled slab dimensions.

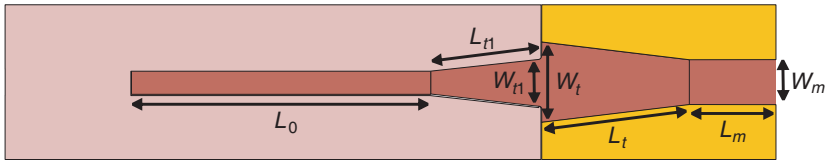

Figure 6. ESIW filter transition and microstrip line, $W_m = 1.93\,\text{mm}$, $L_m = 3.7\,\text{mm}$, $L_t = 6.3446\,\text{mm}$, $W_t = 3.43\,\text{mm}$, $W_{t1} = 2.06\,\text{mm}$, $L_{t1} = 4.6812\,\text{mm}$.

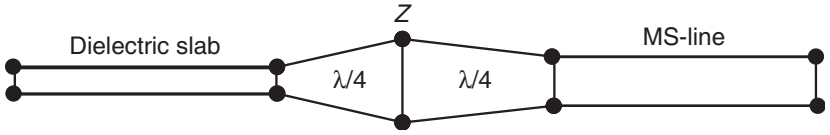

Figure 7. ESIW transition and microstrip line.

displays that tapered transition is formed at microstrip transmission line to connect them together and second tapered transition as well to link dielectric load to microstrip line. Good illustration on ESIW transition to match the impedance of microstrip line to the dielectric slab inside ESIW is displayed in Fig. 7. Waveguide with dielectric slab inside at the centre and its equivalent circuit are found in [19], where impedance difference for both the waveguide and the dielectric slab is introduced.

4. RESULTS OF TRANSMISSION LINE CARICATURIZATION

The designed waveguide shows promising simulated results; therefore, a measurement validation is performed to test the proposed circuit. The simulation results for the waveguide are displayed in Fig. 9. Simulation results fully validate the design procedure stated in this paper, providing a good return loss S_{11} and insertion loss S_{21} (around 0.5-dB). Fig. 8 demonstrates the prototype for presented partially dielectric-filled ESIW. This design is measured using a test fixture and VNA Agilent (8722ES) where the cutoff frequency is around 15 GHz as shown in Fig. 9. Measured insertion loss (S_{21}) is around 2-dB, and return loss (S_{11}) is below $-15\,\text{dB}$ in most of band. Even though the measurement in this frequency band (15–32) GHz is a hard task to maintain, these measured values agree well with simulation.

Phase constant is measured for partially dielectric-filled load by applying Equation (1) to obtain the measured results. The measured phase difference for both lines is obtained and divided on length difference between two transmission lines. In order to measure the phase constant for our proposed ESIW

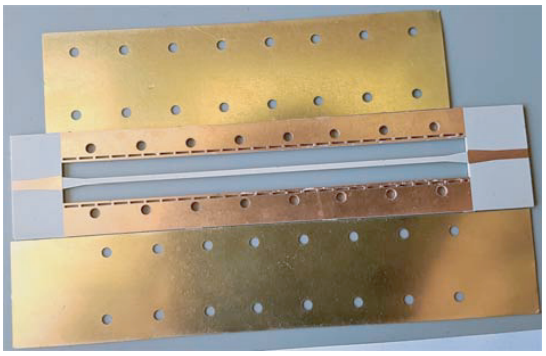

Figure 8. Partially dielectric-filled ESIW prototype.

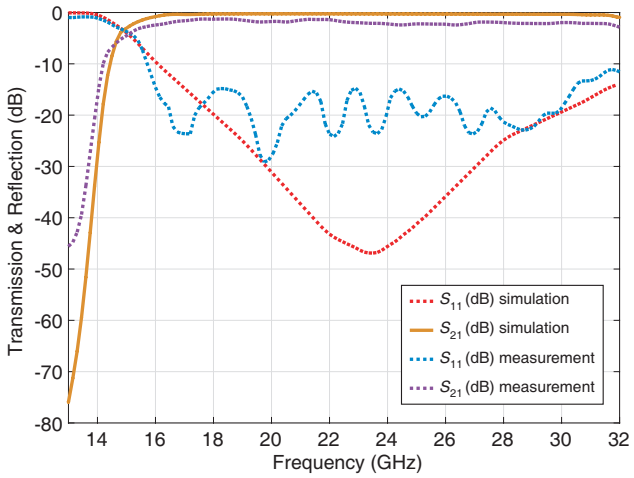

Figure 9. Partially dielectric-filled ESIW return loss (S_{11}) and insertion loss (S_{21}).

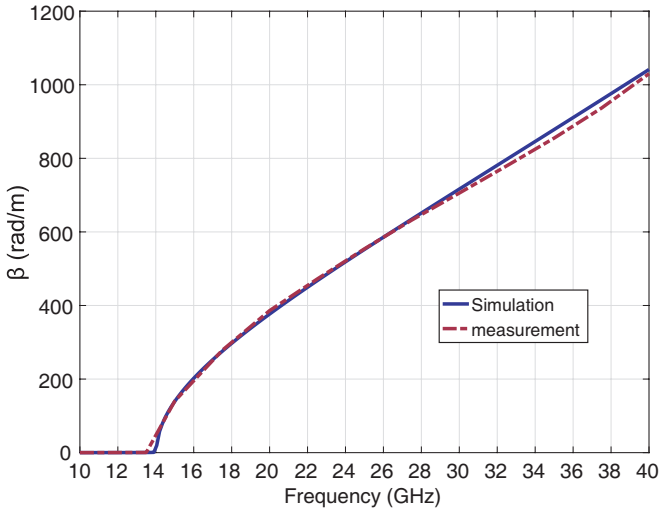

Figure 10. Phase constant of partially dielectric-filled ESIW.

transmission line, two ESIW transmission lines different in length are implemented and measured. After obtaining a pair of S_{21}-parameters for the two differing line sections, the propagation constant is then calculated from the phase difference of the pair of S_{21}-parameters. Equation (1) is used to find the phase constant β for the presented ESIW transmission line in [21].

$$\beta = -\frac{|\angle(S_{21}, \text{long}) - \angle(S_{21}, \text{short})|}{\Delta L} \tag{1}$$

where (S_{21}) is the insertion loss in dB, and ΔL is the length difference between short and long transmission lines.

The measured phase constant β is displayed in Fig. 10. The cutoff frequency for measured β is found around 14.5 GHz where it matches exactly to the simulation. Fluctuation in measured β is noticed around 30 GHz due to the effect of the second mode on the result where the second mode is expected to start around this region. For simulation result, however, we consider only the first mode that can be seen in the curve of simulation. This minor difference in results still exists until 40 GHz where measured and simulated β start to match again very well.

The attenuation constant is measured by readily extracted from Equation (2). In order to accomplish good results, Equation (2) is applied to find the attenuation α where transmission line

with the longer length is divided on the shorter length to examine attenuation α measurements. The attenuation constant is readily extracted from the magnitude difference of the S_{21}-parameters as introduced in [21].

$$\alpha = -\frac{\ln(|S_{21}, \text{long}|/|S_{21}, \text{short}|)}{\Delta L} \tag{2}$$

where (S_{21}) is the insertion loss in dB, and ΔL is the length difference between short and long transmission lines.

In this implementation, the measured and simulated results are illustrated in Fig. 11. This measurement is achieved very good results which agreed well with simulation.

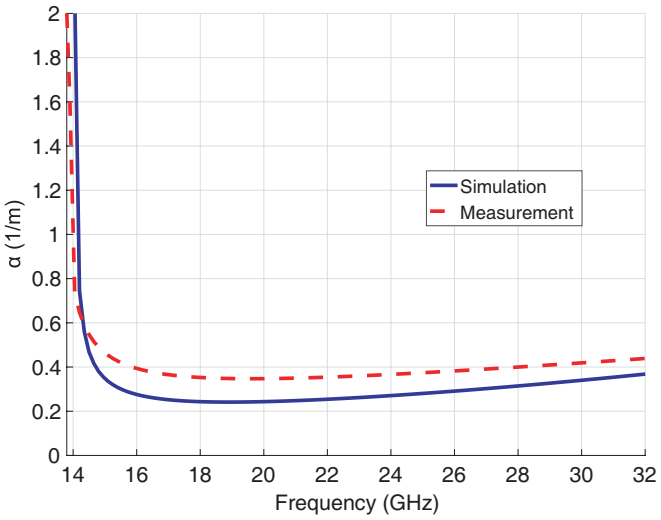

Figure 11. Attenuation simulation and measurement for partially dielectric-filled ESIW.

5. FILTER DESIGN

5.1. Dielectric-Filled Support

The normal waveguide filter with partially dielectric-filled load is required to implement a rectangular dielectric plane in the middle to act as a dielectric load. In planar integrated circuit filter design, the need is increased for building a support for these dielectric loads to create a good possibility for the filter with the loaded dielectric to be designed in planar form. To reduce the number of steps in the fabrication process, this method is introduced with lower cost because the whole circuit is etched on a single planar substrate. This explains the reason behind forming these rectangular supports. The main advantage which is gained from making these supports is opening the possibility of loading a rectangular dielectric load in the planar circuit of the filter. These supports are designed in a way to have less effect on filter performance as shown in Fig. 14. However, losses in terms of dielectric loss still exist. To design solid supports and to satisfy the minimum allowable dimensions in a fabrication process, the filter support width is presented to be equal to 20 mil. It is important to mention that filter support can be designed in different angles to keep the loss to a minimum. The manufacturing process for the introduced filter is achievable because it is done on the same substrate, and a new additional process is added to the fabrication of ESIW.

5.2. Quality Factor of Single Cavity

Single cavity is proposed to study the resonator characteristic for the ESIW filter regarding the quality factor for this kind of cavity filter. A single cavity is weakly coupled through very small accessing rectangular dielectric placed inside ESIW. Fig. 12 demonstrates the single cavity with the rectangular dielectric cavity. The fractional bandwidth is utilized to compute the quality factor by applying the

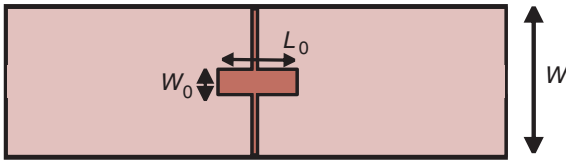

Figure 12. Single cavity with $W = 8\,\text{mm}$, $W_0 = 1\,\text{mm}$, $L_0 = 4\,\text{mm}$.

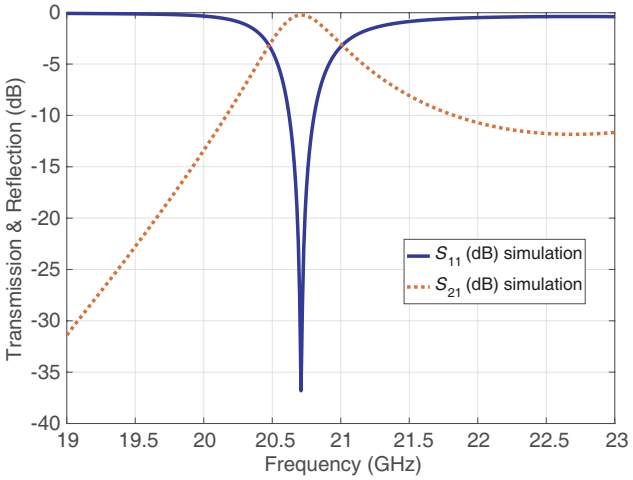

Figure 13. Return loss (S_{11}) and insertion loss (S_{21}) for the proposed cavity.

inverse method to the equation. The unloaded quality factor is calculated for the proposed cavity and lossy rectangular cavity excited with fundamental modes to calculate the quality factor for the designed filter. The quality factor is calculated for a single cavity from SIW single cavity equations in [22].

It can be noticed from Fig. 13 that the fractional bandwidth is around 2.3%. The return loss (S_{11}) and insertion loss (S_{21}) are $-37\,\text{dB}$ and 0.2-dB, respectively. The quality factor for the proposed cavity is calculated equal to 1826 which is better than SIW quality factor. The proposed cavity shows a high quality factor; therefore, filter design is presented as one of the examples for partially dielectric-filled empty PFESIW. From Table 1, the proposed cavity displays a higher quality factor at higher frequency band with lower fractional bandwidth. The resulting values can be directly compared, and they show that the filter presented in this paper is a highly compact solution compared with other recent references in the literature. The quality factor of the presented cavity is higher than the filters of [2, 5, 6], with higher frequency band. Finally, the comparisons in terms of insertion loss and fractional bandwidth show that the cavity presented in this work is better than all the references in Table 1.

Table 1. Comparison of quality factor between previous works and proposed cavity.

Ref.	Freq. (GHz)	Fractional bandwidth (%)	Q. Factor
[2]	19.5	2.56%	1358
[4]	35	2.85%	1085
[5]	15	2.93%	1505
[6]	15	3%	1338
Proposed	20.7	2.3%	1826

5.3. Filter Layout

Bandpass five-poles Chebyshev filter has been designed and measured for millimetre wave applications. The introduced filter has 1.65-GHz bandwidth at center frequency of 21 GHz with 0.1-dB ripple. The filter is simulated and optimized by using available commercial software (HFSS). The substrate of Roger RT 6002 is applied to this filter with permittivity of 2.94, copper thickness of 17 µm, and the thickness of the substrate is 0.762 mm. Invertor resonator filter is realized in ESIW as introduced in Fig. 14. The discontinuities inside ESIW are presented in the centre and supported by 20 mil dielectric supports.

The dimensions of the designed filter are listed in Fig. 14, and it shows that the length of

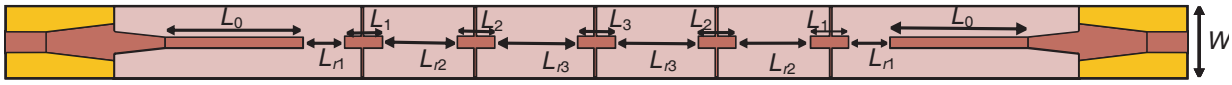

Figure 14. Filter structure with $W = 6.098\,\text{mm}$, $L_0 = 12.77\,\text{mm}$, $L_{r1} = 3.83\,\text{mm}$, $L_1 = 3.56\,\text{mm}$, $L_{r2} = 6.92\,\text{mm}$, $L_2 = 3.475\,\text{mm}$, $L_{r3} = 7.678\,\text{mm}$, $L_3 = 3.518\,\text{mm}$.

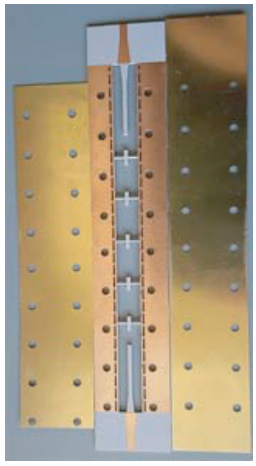

Figure 15. Filter structure prototype.

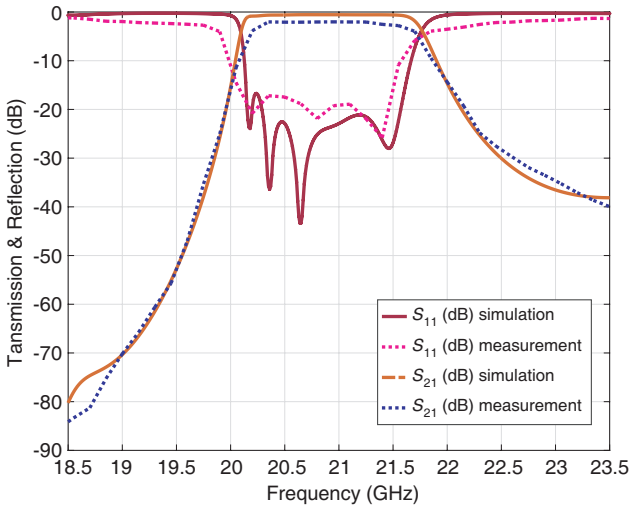

Figure 16. Return loss (S_{11}) and insertion loss (S_{21}).

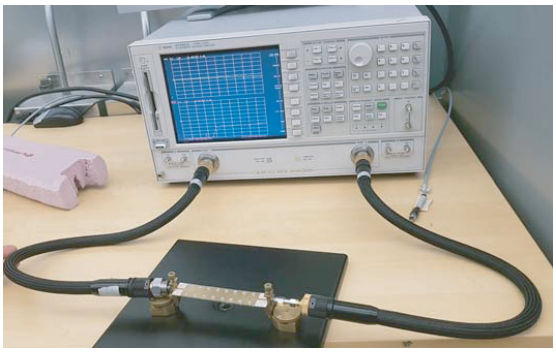

Figure 17. Measurement method for partial-filled waveguide and bandpass ESIW filter.

adoption (L_0) is large compared to the filter invertors where it is connected directly to filter transition. Measurement was done by using a test fixture connected VNA Agilent (8722ES) through RF cables for the designed filter. Test fixture introduced in [20] for testing a planar circuit is shown in Fig. 17. Prior measurement and calibration has been done by using a TRL-kit to optimize the possibility to obtain a smoother result. The test fixture provides a good range of motion to fix the circuits in between two fixtures regardless of the length of the circuit. The test fixture comprises a body adapted to retain therein the planar circuit and is connected to test equipment. Due to the difficulty usually found alongside fabricating ESIW circuits and in our case, dielectric supports are added to PFESIW

fabrication process. The presented dielectric-filled filter is carefully designed to satisfy the fabrication requirements and allowable dimensions ratio specified by manufacturers to fabricate the design as shown in Fig. 15. Although the fabrication challenges are reduced, circuit measurement is hard to perform and needs special care to get results that agree well with simulation. The measured result of the structure exhibits a very good performance and covers range of band from 20.1 to 21.75 GHz (7.85% FBW) with high-frequency selectivity at both band edges which is very good compared to filter introduced in [2]. Moreover, the measured reflection coefficient (S_{11}) is below -20 dB along the passband, and insertion loss (S_{21}) reaches about 1.5 dB at the filter central frequency, with 0.5 dB for simulation. Furthermore, measured out-of-band rejection displays a very sharp cut better than -37 dB at 23.5 GHz. The loss for insertion loss is generated by both the dielectric and conductor losses. The dielectric loss will definitely increase by adding partial dielectric-filled to ESIW. Therefore, quality factor will be decreased for the design. Generally, the partial-filled ESIW still has a higher quality factor than SIW filters design. However, dielectric loss is a bit higher than air-filled ESIW. Some applications will fit perfectly with this dielectric-filled design such as controlling the characteristic impedance of the power divider. This filter offers a flat response with low ripple and low cost where the measurements and simulations agree very well as demonstrated in Fig. 16. It is very essential to mention that by adding the support slabs on both sides of the invertors, filter's higher out-of-band (stop band) curve (S_{21}) for insertion loss becomes sharper and lower. Comparison between the proposed ESIW filter and previous work is presented in Table 2. The partially dielectric-filled PFESIW filter has a smaller size at lower frequency band with less number of poles.

Table 2. Comparison between proposed ESIW filter and previous works.

Ref.	**Number of poles**	f_0 **(GHz)**	**Bands (GHz)**	**Circuit size (mm)**	Substrate (ϵ_r)
Ref. [4]	5	35	34.4–35.4 (2.85%)	30.659×7.11	Rogers 4003C (3.55)
Ref. [5]	5	15	14.8–15.24 GHz (2.93%)	76.5×6	Rogers 4003C (3.55)
Ref. [6]	7	35	34.2–35.6 (4%)	Large multilayer size	Rogers 4003C (3.55)
Proposed	5	21	20.1–21.7 (7.85%)	47.4×6.1	Roger RT 6002 (2.94)

6. CONCLUSION

In this paper, a partially dielectric-filled PFESIW and dielectric loaded filter is presented. The new technique of dielectric-filled PFESIW shows very good performance concerning reducing the size of ESIW and controlling the characteristic impedance where this feature can be very handy for characteristic impedance of power divider. The proposed type of ESIW filter is introduced with a proper transition technique from microstrip to ESIW. Single cavity based on PFSIW technique is presented to calculate the quality factor and to study resonator characteristic for PFESIW. The cavity has shown a very high quality factor better than SIW. The filter displays a very good performance and fabricated on the planar integrated circuit in order to keep the circuit in a simple structure and low cost. The support slabs give the design very good flexibility to be used in planar substrate form. The filter bandwidth at the centre frequency of 21 GHz is 20.1–21.75 GHz. A study of transmission line waveguide is introduced in terms of attenuation, phase constant and characteristic impedance and validated through measurement. The filter's measurement exhibits a very good performance and agrees with simulation very well.

ACKNOWLEDGMENT

The authors would like to express their gratitude to T. Antonescu, Poly-Grames Research Center, École Polytechnique de Montréal, Montréal, QC, Canada, for their support in the realization of the prototypes.

REFERENCES

1. Deslandes, D. and K. Wu, "Integrated microstrip and rectangular waveguide in planar form," *IEEE Microwave and Wireless Components Letters*, Vol. 11, No. 2, 68–70, 2000.
2. Belenguer, A., H. Esteban, and V. E. Boria, "Novel empty substrate integrated waveguide for high-performance microwave integrated circuits," *IEEE Transactions on Microwave Theory and Techniques*, Vol. 62, 832–839, 2014.
3. Mohammadi, P. and S. Demir, "Loss reduction in substrate integrated waveguide structures," *Progress In Electromagnetics Research C*, Vol. 46, 125–133, 2014.
4. Martinez, J. A., J. J. de Dios, A. Belenguer, H. Esteban, and V. E. Boria, "Integration of a very high quality factor filter in empty substrate-integrated waveguide at Q-band," *IEEE Microwave and Wireless Components Letters*, Vol. 28, No. 6, 503–505, Jun. 2018.
5. Borja, A. L., A. Belenguer, H. Esteban, and V. E. Boria, "Design and performance of a high-Q narrow bandwidth bandpass filter in empty substrate integrated coaxial line at Ku-band," *IEEE Microwave and Wireless Components Letters*, Vol. 27, No. 11, 977–979, 2017.
6. Belenguer, A., M. D. Fernandez, J. A. Ballesteros, J. J. de Dios, H. Esteban, and V. E. Boria, "Compact multilayer filter in empty substrate integrated waveguide with transmission zeros," *IEEE Transactions on Microwave Theory and Techniques*, Vol. 66, No. 6, 2993–3000, Jun. 2018.
7. Wegmuller, M., J. P. von der Weid, P. Oberson, and N. Gisin, "Characterization of a dielectric E-plane loaded waveguide by the NMVF: Application to filters design," *Journal of Applied Sciences*, Vol. 7, No. 24, 3983–3988, 2007.
8. Lilonga-Boyenga, D., J. Tao, and T. H. Vuong, "Uniaxial discontinuities analysis by a new multimodal variational methodapplication to filter design," *IEEE Microwave and Wireless Components Letters*, Vol. 17, No. 1, 77–83, 2007.
9. Monsoriu, J. A., B. Gimeno, E. Silvestre, and M. V. Andres, "Analysis of inhomogeneously dielectric filled cavities coupled to dielectric-loaded waveguides: Application to the study of NRD-guide components," *IEEE Transactions on Microwave Theory and Techniques*, Vol. 52, No. 7, 1693–1701, 2004.
10. Yu, C. C. and T. H. Chu, "Analysis of dielectric-loaded waveguide," *IEEE Transactions on Microwave Theory and Techniques*, Vol. 38, No. 9, 1333–1338, Sep. 1990.
11. Belenguer, A., J. L. Cano, H. Esteban, E. Artal, and V. E. Boria, "Empty substrate integrated waveguide technology for E-plane high-frequency and high-performance circuits," *Radio Science*, Vol. 52, No. 1, 49–69, 2017.
12. Ballesteros, J. A., M. D. Fernandez, A. Belenguer, H. Esteban, and V. E. Boria, "Versatile transition for multilayer compact devices in empty substrate integrated waveguide," *IEEE Microwave and Wireless Components Letters*, Vol. 28, No. 6, 482–484, Jun. 2018.
13. Morro, J. V., A. Rodríguez, A. Belenguer, H. Esteban, and V. Boria, "Multilevel transition in empty substrate integrated waveguide," *Electronics Letters*, Vol. 52, No. 18, 1543–1544, Sep. 2016.
14. Parment, F., A. Ghiotto, T. H. Vuong, J. M. Duchamp, and K. Wu, "Air-filled substrate integrated waveguide for low-loss and high power-handling millimeter-wave substrate integrated circuits," *IEEE Transactions on Microwave Theory and Techniques*, Vol. 63, No. 4, 1228–1238, 2015.
15. Díaz-Caballero, E., A. Belenguer, H. Esteban, V. E. Boria, C. Bachiller, and J. V. Morro, "Analysis and design of passive microwave components in substrate integrated waveguide technology," *IEEE Conference on Numerical Electromagnetic and Multiphysics Modeling and Optimization*, 1–3, 2015.
16. Zhang, Y. and W. T. Joines, "Attenuation and power-handling capability of T-septum waveguides," *IEEE Transactions on Microwave Theory and Techniques*, Vol. 35, No. 9, 858–861, 1987.
17. Ding, Y. and K. Wu, "Miniaturized hybrid ring circuits using T-type folded substrate integrated waveguide TFSIW," *IEEE MTT-S International Microwave Symposium Digest*, 705–708, 2009.
18. Khan, A. A., M. K. Mandal, and R. Shaw, "A compact and wideband SMA connector to empty substrate integrated waveguide (ESIW) transition," *IEEE MTT-S in International Microwave and RF Conference (IMaRC)*, 246–248, IEEE, 2015.
19. Marcuvitz, N., *Waveguide Handbook*, No. 21, IET, 1951.

20. Djerafi, T., J. Gauthier, and K. Wu, "Planar circuit test fixture," United States Patent, US2013335110, 2013.
21. Patrovsky, A. and K. Wu, "Substrate integrated image guide (SIIG) — A planar dielectric waveguide technology for millimeter-wave applications," *IEEE Transactions on Microwave Theory and Techniques*, Vol. 54, No. 6, 2872–2879, 2006.
22. Grine, F., T. Djerafi, M. T. Benhabiles, K. Wu, and M. L. Riabi, "High-Q substrate integrated waveguide resonator filter with dielectric loading," *IEEE Access*, Vol. 5, 12526–12532, 2017.